J Bioenerg Biomembr (2015) 47:441–449
DOI 10.1007/s10863-015-9623-y

Gold nanoparticle-mediated (GNOME) laser perforation: a new method for a high-throughput analysis of gap junction intercellular coupling

Daniela Begandt[1] · Almke Bader[1] · Georgios C. Antonopoulos[2] · Markus Schomaker[2] · Stefan Kalies[2] · Heiko Meyer[2,3] · Tammo Ripken[2] · Anaclet Ngezahayo[1,4]

Received: 26 May 2015 / Accepted: 19 August 2015 / Published online: 27 August 2015

Abstract The present report evaluates the advantages of using the gold nanoparticle-mediated laser perforation (GNOME LP) technique as a computer-controlled cell optoperforation to introduce Lucifer yellow (LY) into cells in order to analyze the gap junction coupling in cell monolayers. To permeabilize GM-7373 endothelial cells grown in a 24 multiwell plate with GNOME LP, a laser beam of 88 μm in diameter was applied in the presence of gold nanoparticles and LY. After 10 min to allow dye uptake and diffusion through gap junctions, we observed a LY-positive cell band of 179 ± 8 μm width. The presence of the gap junction channel blocker carbenoxolone during the optoperforation reduced the LY-positive band to 95 ± 6 μm. Additionally, a forskolin-related enhancement of gap junction coupling, recently found using the scrape loading technique, was also observed using GNOME LP. Further, an automatic cell imaging and a subsequent semi-automatic quantification of the images using a java-based ImageJ-plugin were performed in a high-throughput sequence. Moreover, the GNOME LP was used on cells such as RBE4 rat brain endothelial cells, which cannot be mechanically scraped as well as on three-dimensionally cultivated cells, opening the possibility to implement the GNOME LP technique for analysis of gap junction coupling in tissues. We conclude that the GNOME LP technique allows a high-throughput automated analysis of gap junction coupling in cells. Moreover this non-invasive technique could be used on monolayers that do not support mechanical scraping as well as on cells in tissue allowing an in vivo/ex vivo analysis of gap junction coupling.

Keywords Scrape loading · Dye transfer · Gap junction · Gold nanoparticle-mediated laser perforation · GNOME · In vivo · Vascular · Endothelial cells

Daniela Begandt and Almke Bader contributed equally to this publication.

✉ Anaclet Ngezahayo
ngezahayo@biophysik.uni-hannover.de

[1] Institute of Biophysics, Leibniz University Hannover, Herrenhäuser Str. 2, D-30419 Hannover, Germany

[2] Biomedical Optics Department, Laser Zentrum Hannover e. V., Hannover, Germany

[3] Department of Cardiothoracic, Transplantation and Vascular Surgery, Hannover Medical School, Hannover, Germany

[4] Center for Systems Neuroscience Hannover, University of Veterinary Medicine Hannover Foundation, Hannover, Germany

Introduction

Gap junctions are intercellular channels that directly connect the cytoplasm of neighboring cells. They enable the exchange of small molecules (<2 kDa), e. g. metabolites or second messengers. Therefore, gap junction-dependent cell-cell coupling is very important for the communication and coordination of cells in a multicellular tissue (Nielsen et al. 2012; Goodenough and Paul 2009; Harris 2007). Non-functional gap junction channels as a result of specific gene mutations or physiological dysregulation can lead to pre- or postnatal death, as well as severe diseases such as deafness or cataracts (Kelsell et al. 2001; Zoidl and Dermietzel 2010; Figueroa and Duling 2009; Willecke et al. 2002), which demonstrate the importance of gap junctions for tissue homeostasis (Nielsen et al. 2012; Goodenough and Paul 2009).

Intercellular gap junction coupling can be analyzed using the transfer of hydrophilic gap junction permeable dyes such as Lucifer yellow (LY) (Abbaci et al. 2008; el-Fouly et al. 1987). The dye is introduced into a single cell or a limited

number of cells and the subsequent diffusion of the dye through gap junction channels into neighboring cells is evaluated. Dye transfer experiments primarily differ in the method of dye introduction into the cells. The introduction of dye into single cells through microinjection capillaries is an option, which necessitates a micro injector and technical skills that require extensive training (Abbaci et al. 2008). Additionally, the repetitive injection of single cells to achieve a statistically relevant population is a time consuming process. Therefore, the technique is often reduced to proof-of-concept experiments rather than experiments for the quantitative evaluation of gap junction coupling. In contrast, cells grown to a monolayer can be examined by introducing the dye using the scrape loading/dye transfer (SL/DT) technique (Abbaci et al. 2008; el-Fouly et al. 1987). For this method, cells have to be grown to confluence on a hard and even surface such as glass cover slips. In presence of a dye such as LY, the cell monolayer is mechanically scraped with a sharp tool, for instance a razor blade or needle. The dye infiltrates into the cytoplasm of the wounded cells at the edge of the scrape and can diffuse through gap junctions into neighboring cells (Begandt et al. 2010, 2013). The dye diffusion distance within the cell monolayer can then be used for the estimation of gap junction coupling and for a quantitative evaluation of the regulation of gap junction coupling by physiological and pharmacological agents in various cell types (Begandt et al. 2010, 2013; Lee et al. 2010; Xia et al. 2009; Ke et al. 2013).

The SL/DT technique is a simple and convenient method that enables the analysis of gap junction coupling within large cell populations. However, there are also limitations to this method. First, the process of scraping single cover slips is time consuming and necessitates different mechanical steps that can affect gap junction coupling. Second, the geometry of mechanical scrapes varies greatly, which limits the possibility of automation of the imaging and quantification processes. Third, in cells that form a mechanically instable monolayer, the scraping leads to undesirable disruptions of the cell monolayer or a detachment of the cells from the cultivation surface. Therefore, less invasive methods for dye loading, which can be easily automated, are needed to achieve an accurate and high-throughput analysis of gap junction coupling in cell networks. Moreover, a non-invasive technique promises the possibility of gap junction coupling analysis in three dimensional (3D) tissues in and/or ex vivo.

Various laser perforation (optoperforation) techniques promise to be new cell friendly permeabilization methods that allow the uptake of various molecules into cells, while not affecting the cellular viability (Stevenson et al. 2010). A high-throughput variant of the laser perforation technique is the gold nanoparticle-mediated (GNOME) laser perforation (Schomaker et al. 2010; Heinemann et al. 2013; Kalies et al. 2014). During GNOME laser perforation (GNOME LP), the cell permeabilization is induced by heating effects generated by a laser beam weakly focused at gold nanoparticles (diameter 200 nm) that are adhered on the cell membrane. To date, GNOME LP has been successfully used for the cellular introduction of dextran-coupled dyes as well as siRNA and morpholinos into different cell types (Heinemann et al. 2013; Kalies et al. 2013, 2014; Schomaker et al. 2014). During these experiments, it could be shown that the permeabilization of the cells supported a cell viability of more than 90 %. We propose to adapt the GNOME LP method to a GNOME LP/dye transfer (GNOME LP/DT) technique that can be used to analyze intercellular gap junction coupling in cell monolayers. This technique will offer many advantages, such as the avoidance of mechanical invasiveness, the possibility of automated cell permeabilization, cell imaging as well as experiment evaluation. Additionally we applied the GNOME LP/DT technique to 3D cultivated cells to test the in vivo/ex vivo applicability of the method.

Materials and methods

Chemicals

Carbenoxolone (CBX), forskolin, Hoechst 33342, tetramethylrhodamine isothiocyanate (TRITC)-dextran, average weight 4.4 kDa, and Lucifer yellow (LY) were purchased from Sigma-Aldrich (Munich, Germany). Gold nanoparticles (AuNP, 7×10^8 particles/ml) with a size of 200 nm were delivered from Kisker Biotech (Steinfurt, Germany). For dye transfer experiments, cells were cultivated for 6 h in presence of forskolin (100 μM) or DMSO (0.2 %). Untreated cells and cells treated with dimethylsulfoxide (DMSO), which was used in all experiments as vehicle for forskolin, served as reference.

Cell culture

Bovine GM-7373 aortic endothelial cells (Deutsche Sammlung von Mikroorganismen und Zellkulturen GmbH, Braunschweig, Germany) were cultivated using Dulbecco's Modified Eagle's/Ham's F-12 Medium (DMEM/Ham's F-12, Biochrom, Berlin, Germany) and the rat brain endothelial cell line RBE4 was cultivated with a mixture of Ham's F-10 and alpha-MEM medium (Biochrom). Both media were supplemented with 10 % fetal calf serum (FCS), penicillin and streptomycin (100 U/ml and 0.1 mg/ml, respectively). Additionally, basic fibroblast growth factor (Sigma-Aldrich) with a final concentration of 1 ng/ml was added to the RBE4 medium. The cultures were maintained at 37 °C in a cell culture incubator with a humidified atmosphere containing 5 % CO_2. The culture medium was renewed every 2–3 days.

Scrape Loading/Dye Transfer (SL/DT)

For SL/DT experiments, cover slips (Ø 10 mm) were placed into the wells of a 24 multiwell plate containing 0.5 ml of the corresponding culture medium. The cells were seeded at a density of about 4×10^5 cells/well. Additional cultivation for 24–48 h allowed the cells to adhere and form a monolayer on the cover slip. Analyses of functional gap junction coupling were performed using the SL/DT technique as previously described (Begandt et al. 2010). Briefly, the cells were washed with a bath solution containing 121 mM NaCl, 5.4 mM KCl, 6 mM $NaHCO_3$, 5.5 mM glucose, 0.8 mM $MgCl_2$, 1 mM EGTA, and 25 mM HEPES (pH 7.4, 295 mOsmol/l). The scrape was introduced with a razor blade in presence of 0.25 % LY dissolved in bath solution and incubated for 10 min. Afterwards the cells were washed twice with the bath solution containing 1.8 mM $CaCl_2$. The cells were fixed for 10 min in 4 % formaldehyde dissolved in phosphate buffer saline (PBS) composed of 137 mM NaCl, 2.8 mM KCl, 10 mM Na_2HPO_4 and 1.8 mM KH_2PO_4 (pH 7.4, 295 mOsmol/l) and were stored in PBS for further microscopic analysis. In CBX (100 μM) experiments, the chemical was also present during the scraping and washing steps.

Gold Nanoparticle-mediated Laser Perforation/Dye Transfer (GNOME-LP/DT)

For GNOME LP/DT experiments, the cells were seeded at a density of about 4×10^5 cells/well in a 24 multiwell plate and were cultivated for 24–48 h until they reached confluence. Prior to the experiments, AuNP (0.5 $\mu g/cm^2$) were added to the cells for 3–6 h to allow the particles to adhere onto the cell surface. A modified SL/DT protocol was used for the GNOME LP/DT experiments. The cells were washed with the bath solution as described for SL/DT and then were laser-permeabilized in the presence of 0.25 % LY alone or with 0.4 % TRITC-dextran dissolved in bath solution. The laser system set-up and laser treatment was performed according to Heinemann et al. (2013). The set-up included a 532 nm Nd:YAG microchip laser (Horus Laser, Limoges, France), enabling 850 ps laser pulses with a repetition rate of 20 kHz, a telescope for the adjustment of the laser diameter and a half-wave plate combined with a polarizing beam-splitter (Thorlabs, Newton, USA) for adjustment of the laser power. A motorized stage (Carl Zeiss, Jena, Germany) with controller unit (Prior Scientific, Cambridge, UK) and a scanner (Müller Elektronik, Spaichingen, Germany) enabled the positioning and scanning of the multiwell plates. The laser power and the scanning velocity as well as the selection of individual wells were controlled by a self-developed, LabView-based software (Heinemann et al. 2013). To perform GNOME LP/DT, in each well of a 24 multiwell plate, a line of cells was optoperforated by a 35 mW laser beam of 88 μm in diameter with a scanning velocity of 40 mm/s. After variable dye diffusion times, the cells were washed twice with fresh Ca^{2+}-containing bath solution as described above for manual SL/DT experiments. The fixation and conservation of the cells were performed as described for SL/DT experiments. In CBX experiments, the chemical was also present during the optoperforation and the washing steps.

Quantification of SL/DT Experiments

The SL/DT experiments were documented with a confocal laser scanning microscope (Nikon, Düsseldorf, Germany) using the software program EZ-C1 3.50 (Nikon). A view area of 1024 × 1024 pixels (1273 × 1273 μm) was recorded. The settings for gain, brightness and contrast were not changed for all images within a set of experiments and no editing of the images occurred prior to quantification. The estimation of the dye transfer was performed with the software ImageJ (http://rsbweb.nih.gov/ij/docs/menus/analyze.html) as previously described (Begandt et al. 2010). Briefly, the dye diffusion distance was calculated on the basis of plot profiles generated along the scrape from which the background brightness was subtracted. Per cover slip four micrographs each with six frames with a size of 300 × 100 pixels (length × width) were analyzed with a MATLAB-based software (Begandt et al. 2010). For each treatment, at least four experiments were performed from which the average dye diffusion distance and SEM were calculated.

Quantification of GNOME LP/DT Experiments

To automatically document the GNOME LP/DT experiments, images were obtained with an Orca Flash 4.0 camera (Hamamatsu Photonics, Herrsching am Ammersee, Germany) mounted onto an Eclipse Ti microscope (Nikon) using the NIS elements AR 4.21 software (Nikon). The tool Multipoint ND acquisition was used to generate three images with 2048 × 2048 pixels (3367 × 3367 μm) per well. Two images documented the dye uptake and diffusion in the cells and one image was obtained away from the perforation line, which documented a section of cells that did not contain the dye. The latter image was used for estimation of the background. A constant exposure was used for all images. The automatic focus module of the Eclipse Ti microscope was used to keep the cells in focus during the automatic imaging of the cells in the wells. To analyze the data obtained through the automatic documentation of the 24 multiwell plate, a Java-based ImageJ-plugin was designed which omitted the manual generation of the plot profiles by allowing a robust and automatic detection of the dye-infiltrated cell region in a set of fluorescence images. The plugin detected the boundary of the fluorescent cell band and performed an average intensity projection along the direction of the band. Furthermore, the plugin provided an

alert for detecting image artifacts and outliers in the dye-loaded cell area, allowing the user to correct the boundary of the cell band if necessary. The results were passed to the MATLAB-based software described in a previous publication (Begandt et al. 2010) for calculation of the dye diffusion distance. For each treatment, the average dye diffusion distance and SEM from at least six experiments (at least four passages) were calculated.

Three-dimensional cultivation of cells

To allow the GM-7373 cells to form a 3D pseudo capillary, the cells were introduced into glass capillaries with an inner diameter of 0.58 mm or 1.1 mm, respectively. The cells were allowed to proliferate and to cover the inner surface of the capillaries for 48 h. The AuNP were introduced in the capillaries and allowed to adhere onto the cells for at least 3 h. To avoid an inhomogeneous distribution of the particles the glass capillaries were gently agitated during the AuNP incubation period. A LY-containing bath solution was introduced into the capillaries using a small pipette tip and the capillaries were placed in the GNOME set-up for optoperforation as described above. After washing and fixation of the cells the nuclei were stained with Hoechst 33342. Images of the cells grown in the capillaries were generated using the z-stack tool of the EZ-C1 software and the volume render tool of the software EZ-C1 Free Viewer (Nikon). The dye diffusion distance in untreated cells was compared to that found in cells permeabilized in the presence of CBX.

Statistical analysis

All experiment sets were performed in at least three cell passages. For statistical analyses, a paired two-sample Student's *t*-test was used. The significance is given as * for $P < 0.05$, ** for $P < 0.01$ and *** for $P < 0.001$ for at least four experiments for each treatment.

Results

Gap junction coupling analysis: comparison between SL/DT and GNOME LP/DT

The analysis of gap junction-dependent intercellular coupling is often performed by the SL/DT technique (Abbaci et al. 2008; el-Fouly et al. 1987; Begandt et al. 2010). This simple technique can be used to access the degree of gap junction coupling and to screen the effect of various substances on gap junction coupling in different cells (Fig. 1) (Begandt et al. 2010, 2013). In GM-7373 endothelial cells, a LY diffusion distance of approximately 142 ± 2 μm was measured 10 min following the onset of the SL/DT experiment (Fig. 1b). The presence of the gap junction channel blocker CBX during SL/DT reduced the dye diffusion distance to 57 ± 3 μm (paired Student's *t*-test, compared to untreated cells; df = 5, $t = 32.08$, $P = 5.5 \times 10^{-7}$), which represents the first row of cells that were injured during scraping (Fig. 1b). The comparison between the results obtained in the absence or presence of the gap junction blocker CBX clearly indicates that the lateral diffusion distance of the LY of 85 ± 3 μm in the untreated cell monolayer was due to gap junction coupling. Conversely, the SL/DT experiments showed that the adenylyl cyclase activator forskolin significantly increased gap junction coupling of the GM-7373 endothelial cells (Fig. 1b). In cells cultivated in the presence of forskolin for 6 h before SL/DT experiments, a dye diffusion distance of 165 ± 2 μm was observed after a diffusion time of 10 min (paired Student's *t*-test, compared to DMSO-treated cells; df = 5, $t = -12.61$, $P = 5.6 \times 10^{-5}$). This increase in the diffusion distance was solely due to a forskolin-dependent action on gap junction coupling and did not involve DMSO, which was also present (0.2 %) in the experiments. In cells that were cultivated for 6 h with DMSO only, a diffusion distance of 137 ± 3 μm was observed (Fig. 1b, paired Student's *t*-test, compared to untreated cells; df = 5, $t = 1.32$, $P = 0.25$). After subtraction of the value found when SL/DT was performed in presence of CBX, the dye diffusion distance found in cells treated with forskolin and DMSO alone was 108 ± 4 μm and 80 ± 4 μm, respectively, indicating a forskolin-related enhancement of the gap junction coupling of 135 %.

We tested whether optoperforation-based GNOME LP could be used to introduce the dye into the cells to allow the analysis of gap junction coupling in cell monolayers establishing thereby a new method named GNOME LP/dye transfer (GNOME LP/DT). In our experimental set-up the GNOME LP/DT uses a laser beam with a diameter of 88 μm, which, by interacting with large gold nanoparticles (Ø 200 nm) in vicinity of the cell membrane, permeabilizes the plasma membrane (Heinemann et al. 2013; Kalies et al. 2014). It has been shown before that gold nanoparticles with a size of 200 nm are best suited for the cell friendly delivery of several substances, for example dextrans or siRNA (Kalies et al. 2013). With the GNOME LP/DT LY was introduced into the GM-7373 endothelial cells. As in SL/DT experiments, the cells were allowed to laterally transmit LY for 10 min after the GNOME LP process. A 179 ± 8 μm wide band of LY-positive cells was found (Fig. 2). The width of the LY-positive cell band was reduced to 112 μm when the cells were fixed immediately after the GNOME LP/DT process without allowing additional time for dye diffusion. The width of the LY-positive cell band was increased to 267 μm when the diffusion time following laser application was changed to 15 min (Fig. 2a). Additionally, when the gap junction blocker CBX was present during GNOME LP/DT experiments a dye diffusion distance of only 95 ± 6 μm was found corresponding to approximately 2–3

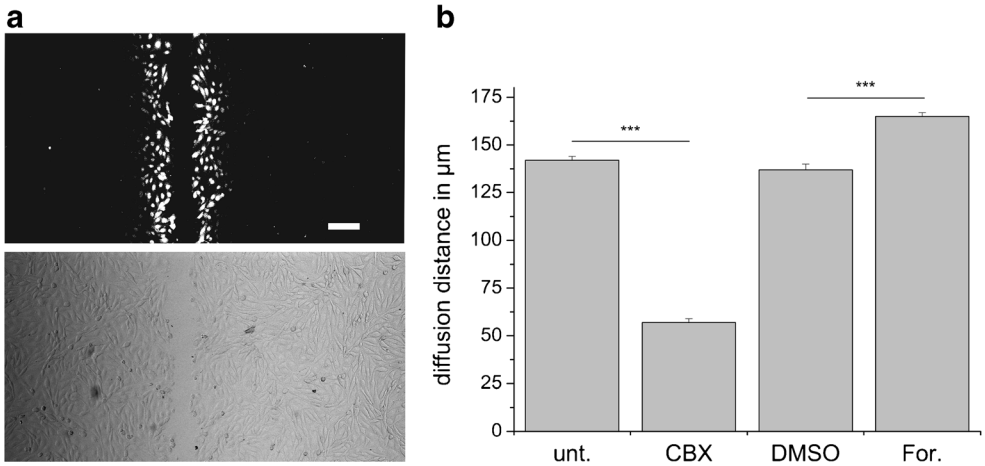

Fig. 1 SL/DT experiment with endothelial GM-7373 cells using the fluorescent dye LY. **a** A typical fluorescent micrograph and correspondent differential interference contrast (DIC) image of cells loaded with LY. **b** Quantitative evaluation of SL/DT experiments performed on cells cultivated with forskolin (For.), DMSO, and under control conditions, as well as cells treated with carbenoxolone (CBX). Cultivation of the cells with forskolin (100 μM) for 6 h increased the dye diffusion distance compared to cultivation of the cells with DMSO (0.2 %), which was used as the solvent for forskolin. Results are shown as average ± SEM from at least four experiments, asterisks indicate $P < 0.001$. The scale bar represents 100 μm

rows of cells (Fig. 2b, paired Student's *t*-test, compared to untreated cells; df = 3, $t = 12.61$, $P = 1.1 \times 10^{-3}$). The results indicate that when gap junction channels were blocked by CBX, LY entered only into the cells that were within the laser beam. Similarly, we performed GNOME LP/DT in the concomitant presence of LY and a gap junction impermeable TRITC-dextran (4.4 kDa). While LY diffused through the gap junctions into the cells that were not within the range of the laser beam, TRITC-dextran was only found in the cells that were directly permeabilized by the laser beam (Fig. 2c). It is striking that the band of the TRITC-dextran-positive cells had the same width as the band of the LY-positive cells found when LY was introduced into CBX-treated cells (Fig. 2c). The results indicate that the LY-positive cell band larger than 95 μm that was found when GNOME LP/DT was performed in the absence of CBX (Fig. 2b) corresponded to a lateral diffusion of LY through gap junction channels in the cell monolayer. For a diffusion time of 10 min, this dye diffusion distance in the monolayer of untreated cells related to gap junction coupling was found to be 83 ± 7 μm.

The SL/DT technique showed that forskolin enhanced the gap junction coupling in GM-7373 endothelial cells (Fig. 1; Begandt et al. 2010). We therefore tested whether GNOME LP/DT, could also detect this forskolin-related effect. We performed GNOME LP/DT on cells cultivated for 6 h in the presence of forskolin and allowed a dye diffusion for 10 min. The width of the LY-positive cell band was found to be 239 ± 11 μm (Fig. 2b, paired Student's *t*-test, compared to DMSO-treated cells; df = 3, $t = -8.27$, $P = 3.7 \times 10^{-3}$). Notably, DMSO did not affect the gap junction coupling (paired Student's *t*-test, compared to untreated cells; df = 3, $t = 1.62$, $P = 0.20$). A 166 ± 4 μm wide LY-positive cell band was observed in cells cultivated for 6 h with DMSO (0.2 %) (Fig. 2b). Similar to the SL/DT experiments, the 95 μm wide band of LY-positive cells, which represents the cells directly permeabilized by the laser beam as shown by application of GNOME LP/DT in presence of CBX, was subtracted from the measured dye diffusion distance observed in all other experiments. Relative to the cells cultivated in the presence of DMSO (70 ± 6 μm), cell cultivation with forskolin for 6 h increased the dye diffusion distance to 143 ± 9 μm, which correlates to an enhancement of the gap junction coupling of 203 %.

GNOME LP/DT opens new possibilities to high throughput screening

As mentioned above, one limitation of the SL/DT technique is the geometric variability of the mechanic scrape, which hinders the automation of experiment processing (Fig. 1). Using GNOME LP/DT, we could generate an accurate band of LY-positive cells (Fig. 2), allowing the automatic imaging and the implementation of a subsequent semi-automatic evaluation of the images using an ImageJ-plugin. The GNOME LP/DT-treated multiwell plate was mounted on a motorized microscope table. Subsequently, the fluorescent images of each well of the 24 multiwell plate were obtained using a multipoint memory tool. The images were further processed with a custom-made ImageJ-plugin based on Java. Using this tool, the dye diffusion plot profiles (Begandt et al. 2010) were automatically generated and saved. These data were passed to the homemade MATLAB-based software described for the SL/DT experiments, which then calculated the dye diffusion distance.

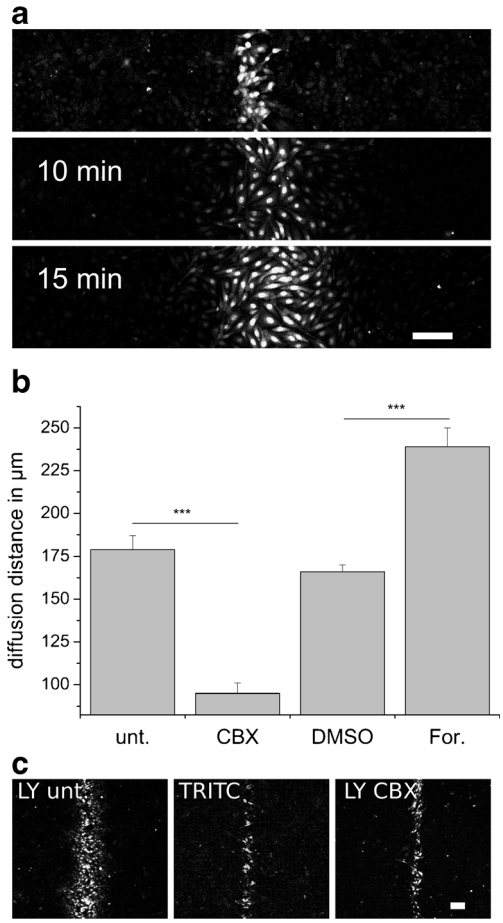

Fig. 2 Analysis of gap junction coupling of GM-7373 cells using GNOME LP/DT. **a** Fluorescent micrographs of LY-loaded cells using GNOME LP/DT. The width of the LY-positive cell band increased with the diffusion time following the GNOME LP/DT process. **b** For quantification, a diffusion time of 10 min was selected. In cells that were cultivated in the presence of forskolin (For., 100 μM) for 6 h, GNOME LP/DT revealed an increase of the diffusion distance compared to cells cultivated with DMSO (0.2 %). **c** Concomitant introduction of LY (left) and TRITC-dextran (center) using GNOME LP/DT. The band of TRITC-dextran-positive cells was narrow compared to the band of LY-positive cells. It is striking that the band of TRITC-dextran-positive cells was comparable to that of LY-positive cells observed when LY was introduced into the cells in presence of CBX (right). The quantitative results in **b** are given as average from at least six experiments ± SEM, asterisks indicate $P < 0.001$. Scale bars represent 100 μm

GNOME LP/DT increases the number of investigable cell types and tissues

Another major limitation of the SL/DT technique is that for some cell types, such as HUVEC or RBE4 cells, we observed that during SL/DT, the cells at the edge of the scrape were squeezed or shredded, rendering an estimation of the dye diffusion distance in the monolayer very difficult (Fig. 3a). As an optical method, GNOME LP/DT did not alter the mechanical adhesion of the cells on the culture surface. Because the detachment of the cells could be avoided, an evaluation of the gap junction coupling in RBE4 cells was possible. Using the optoperforation-based GNOME LP/DT, we found LY-loaded RBE4 cells with a width of 178 ± 11 μm under control conditions (Fig. 3). The width of the LY-positive cells was reduced to 101 ± 5 μm when the GNOME LP process was performed in the presence of the gap junction inhibitor CBX (Fig. 3).

The SL/DT technique can only be applied on cells growing in 2D. We tested whether the GNOME LP/DT could be applied to 3D tissues such as blood vessels. Pseudo vessels were generated by cultivation of the GM-7373 cells in glass capillaries. First it is striking that the cells were able to grow and line the inner surface of the glass capillaries imitating a vessel lumen (Fig. 4). This allowed us to introduce the AuNP into the pseudo vessels and to perform GNOME LP/DT (Fig. 4a). Using GNOME LP/DT we found a LY-positive cell band of approximately 160 μm indicating that cells which were not located within the width of the laser beam (Ø 88 μm) were able to acquire the dye from neighboring cells by diffusion through gap junctions (Fig. 4b). Furthermore, the width of the LY-positive cells was clearly reduced in CBX-treated cells (Fig. 4b). These experiments give evidence that GNOME LP/DT could be applied to 3D tissues.

Discussion

Gold nanoparticle-mediated laser perforation (GNOME LP) was previously found as a cell friendly rapid method to deliver substances, for example dextrans or siRNA into cells (Heinemann et al. 2013; Kalies et al. 2013). In the present report we show the method can also be used to introduce gap junction permeable dyes into cells to evaluate the level of gap junction coupling in the cell monolayer (Fig. 2). Our experimental set-up with a laser beam of 88 μm, which, by interacting with large gold nanoparticles (Ø 200 nm) in vicinity of the cell membrane, permeabilizes the plasma membrane (Heinemann et al. 2013; Kalies et al. 2013, 2014) allowed the uptake of the dye, which then diffused laterally in the cell monolayer through gap junctions. After a diffusion time of 10 min, a LY-positive cell band of 179 μm was observed. The lateral diffusion through gap junctions was demonstrated by experiments in which the GNOME LP/DT was applied in presence of the gap junction blocker CBX (Fig. 2). CBX reduced the LY-positive cell band to 95 μm (2–3 cell rows) corresponding to the cells which were directly permeabilized by the laser beam of about 88 μm. The observation that when GNOME LP/DT was applied in presence of both the gap junction permeable LY and the gap junction impermeable 4.4 kDa TRITC-dextran, LY diffused laterally while the dextran stayed constrained in a cell band of about 90 μm also supports our assumption that the laser permeabilized the cells, which then absorbed the dye in the external solution. These

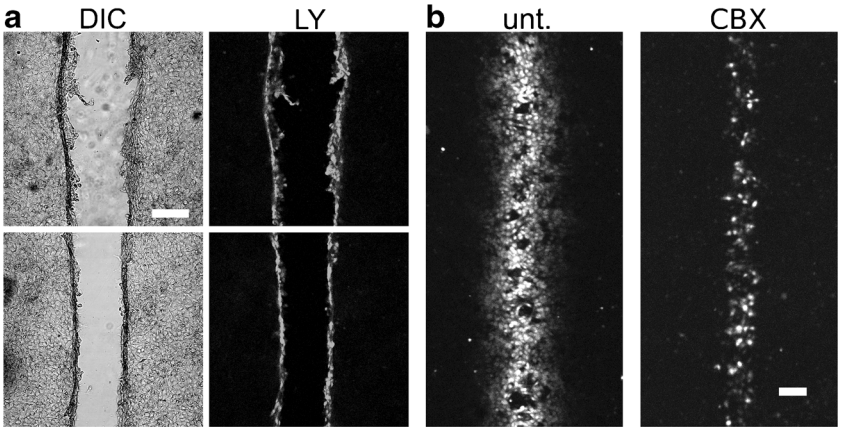

Fig. 3 Analysis of gap junction coupling in RBE4 cells using SL/DT and GNOME LP/DT. **a** Micrographs of RBE4 cells showing undesirable disruptions, such as shredded (upper section) or squeezed (lower section) cells at the edge of the scrape, as result of mechanical scraping. Consequently, the dye diffusion distance could not be estimated. LY fluorescence is shown in white and the cells were additionally imaged with the differential interference contrast (DIC). **b** The LY uptake and diffusion in RBE4 cells revealed by GNOME LP/DT. The width of the band of LY-positive cells was reduced when GNOME LP/DT was performed in the presence of CBX. Scale bars represent 100 μm

cells transmitted the dye laterally through gap junctions if the dye was gap junction permeable.

Using SL/DT, we recently showed that forskolin and other stimulators of cAMP production were able to enhance the gap junction coupling in GM-7373 cells (Begandt et al. 2010; Fig.1). A forskolin-related enhancement of the gap junction coupling could also be reproduced using the GNOME LP/DT

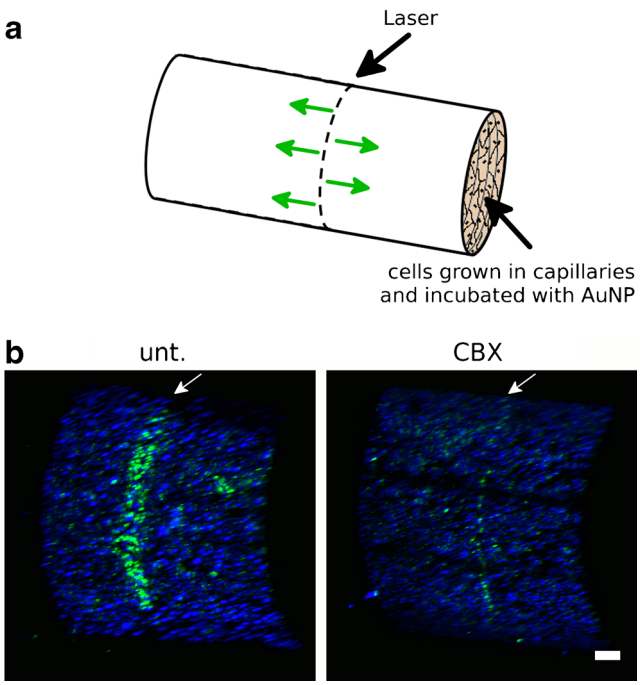

Fig. 4 **a** Schematic representation of GM-7373 cells grown in glass capillaries. Arrows indicate the expected direction of the dye diffusion. **b** Section of a three-dimensional microscopic image of GM-7373 cells in a glass capillary (inner diameter: 1.1 mm) after GNOME LP/DT. The band of LY-positive cells (arrows) can be clearly recognized. CBX reduced the width of the LY-positive cell band. Cell nuclei were stained with Hoechst 33342 (blue) for better visualization of the cells. Scale bar represents 100 μm

(Fig. 2). We show that while DMSO, which was used as vehicle for forskolin, did not influence the gap junction coupling compared to control conditions, the cultivation of the cells in presence of forskolin increased the dye diffusion distance in the monolayers (Fig. 2). Relative to the cells cultivated in the presence of DMSO, cell cultivation with forskolin for 6 h enhanced the gap junction coupling up to 203 % (Fig. 2). It is striking that the effect of forskolin observed using GNOME LP/DT is reinforced compared with the effect observed using the mechanical SL/DT (Begandt et al. 2010; Fig.1). The interpretation for this observation is that GNOME LP/DT may be less invasive for the cells. Performing dye loading or transfection using optoperforation techniques such as GNOME LP, it was shown that the loading of the cells with molecules present in the extracellular milieu was compatible with a cell viability of up to 90 % (Kalies et al. 2014; Baumgart et al. 2012). How the mechanical SL/DT affects the viability of the injured cells is not known, but from the observation of the cells on the edges of the mechanical scrapes, it can be speculated that many injured cells die before they transfer the dye into neighboring cells. It has been shown that mechanically damaging tissues rapidly reduces the gap junction coupling in the affected cells (Carbone et al. 2014). Therefore, we assume that the invasive SL/DT technique underestimates the degree of gap junction coupling in a cell monolayer and most likely leads to underestimation of the regulating effect of physiological and pharmacological agents on the gap junction coupling. Collectively, our results show that GNOME LP/DT can advantageously replace mechanical SL/DT for the analysis of gap junction coupling in cell monolayers.

As mentioned above, the geometric variability of the mechanic scrape produced during SL/DT experiment (Fig. 1) hinders the automation of experiment processing. During GNOME LP/DT experiments, the cell permeabilization is

achieved by a laser beam which interacts with nanoparticles in close vicinity of the cell membrane (Heinemann et al. 2013; Kalies et al. 2013, 2014). By reducing the mechanical intervention of the experimenter, an accurate band of LY-positive cells (Fig. 2) was produced in cell monolayers cultivated in the wells of a 24 multiwell plate, which could then be automatically imaged and evaluated using a java-based ImageJ-plugin. This automation offers the corollary advantage of rapidity and avoidance of experimenter-related biases. The automatic plot profile generation of the three fluorescent images per well of a 24 multiwell plate, the transfer of the images to the MATLAB software and the evaluation of the dye diffusion distances in a complete excel table were accomplished within 30 min. To generate and evaluate the same amount of data using the traditional scrape loading method (Begandt et al. 2010, 2013), required more than 3 h and necessitated the continuous presence of an experimenter. Moreover, the automation can still be improved by integrating the washing and fixation steps, as well as optics for fluorescence imaging and further documentation in the GNOME laser apparatus.

Because of the invasiveness of the SL/DT technique, we found that cells such as HUVEC or RBE4 cells could not be studied. They formed monolayers which were destroyed during the SL/DT process (Fig. 3a). The GNOME LP/DT as an optic-based method did not alter adhesion of the cells on the culture surface, rendering possible the estimation of gap junction coupling in these cells. As shown in Fig. 3, after application of GNOME LP/DT technique a band of LY-loaded RBE4 cells with a width of 178 μm could be found after a diffusion time of 10 min. The width of the LY-positive cells was reduced to 101 μm when the gap junction inhibitor CBX was present during the GNOME LP/DT process, clearly indicating that gap junction coupling was necessary for a lateral diffusion of the dye in the RBE-4 cell monolayer.

The SL/DT technique is used on cells cultivated in 2D on hard and even materials such as glass cover slips. We show in this report that the GNOME LP/DT technology can be applied on cells grown in 3D. As shown in Fig. 4, cells which formed a 3D pseudo vessel when cultured in glass capillaries could be addressed by GNOME LP/DT. It is shown that the width of the band of LY-positive cells could be reduced by the gap junction inhibitor CBX, clearly indicating that the method can be used to access the degree of gap junction coupling in 3D structures. These experiments open a possibility to analyze gap junction coupling in 3D tissue and even in living animal tissues such as blood vessels. The vascular cells exhibit homocellular gap junction coupling between the endothelial cells and between the smooth muscle cells as well as heterocellular gap junctions between the endothelial and the surrounding smooth muscle cells (Figueroa and Duling 2009). The analysis of the gap junction coupling in 3D tissue structures would appreciably increase our understanding of the role played by gap junctions in the physiology of various tissues such as the heart, the brain and the blood vessels (Nielsen et al. 2012; Goodenough and Paul 2009; Figueroa and Duling 2009). However, physiological assays to access the coupling in 3D structures are still missing. Using our pseudo vessels, we show that the GNOME LP/DT could be applied on 3D tissues for example isolated, dissected vessels for ex vivo investigations or direct in vivo studies. However, some improvements for an optimal in vivo usage are still required. The application set-up for in vivo investigations will need adaptation to tissues and animals. The accessibility of the AuNP, the excitatory laser beam as well as the imaging system to deep layers in the tissue are issues that will need new considerations. While the introduction of the AuNP to cell layers in tissue still is a challenging issue, the excitation of the AuNP and imaging in deep layers of tissue can be solved, at least to a certain extent, by the usage of multiphoton systems (Werkmeister et al. 2007; Osswald and Winkler 2013).

In conclusion, we show that GNOME LP/DT is a fast and reliable method for high-throughput analyses of gap junction coupling in different cell types. Unlike SL/DT, GNOME LP/DT does not require the cultivation of the cells on a hard and even surface. The technique can therefore be used to analyze gap junction coupling of cells cultivated in 3D or on softer materials, e. g. matrigel. Additionally, the scanning parameters (power of the laser beam and the scanning velocity) can be adapted to different cell types and to specific cultivation conditions. Moreover, by adapting the application unit, the technology could be used for analysis of gap junction coupling in tissue even in vivo.

Acknowledgments The authors thank Dr. Sabrina Schlie-Wolter for the kind gift of the RBE4 cells. The authors also thank Kristina Schmitt and Anne Klett for their assistance with the experiments.

References

Abbaci M, Barberi-Heyob M, Blondel W, Guillemin F, Didelon J (2008) Advantages and limitations of commonly used methods to assay the molecular permeability of gap junctional intercellular communication. Biotechniques 45(33–52):56–62. doi:10.2144/000112810

Baumgart J, Humbert L, Boulais É, Lachaine R, Lebrun J, Meunier M (2012) Off-resonance plasmonic enhanced femtosecond laser optoporation and transfection of cancer cells. Biomaterials 33: 2345–2350. doi:10.1016/j.biomaterials.2011.11.062

Begandt D, Bader A, Dreyer L, Eisert N, Reeck T, Ngezahayo A (2013) Biphasic increase of gap junction coupling induced by dipyridamole in the rat aortic a-10 vascular smooth muscle cell line. J Cell Commun Signal 7:151–160. doi:10.1007/s12079-013-0196-4

Begandt D, Bintig W, Oberheide K, Schlie S, Ngezahayo A (2010) Dipyridamole increases gap junction coupling in bovine GM-7373 aortic endothelial cells by a cAMP-protein kinase a dependent pathway. J Bioenerg Biomembr 42:79–84. doi:10.1007/s10863-009-9262-2

Carbone SE, Wattchow DA, Spencer NJ, Hibberd TJ, Brookes SJ (2014) Damage from dissection is associated with reduced neuro-musclar transmission and gap junction coupling between circular muscle

cells of guinea pig ileum, *in vitro*. Front Physiol 5:319. doi:10.3389/fphys.2014.00319

el-Fouly MH, Trosko JE, Chang CC (1987) Scrape-loading and dye transfer. A rapid and simple technique to study gap junctional intercellular communication. Exp Cell Res 168(2):422–430

Figueroa XF, Duling BR (2009) Gap junctions in the control of vascular function. Antioxid. Redox Signal. 11:251–266. doi:10.1089/ars.2008.2117

Goodenough DA, Paul DL (2009) Gap junctions. Cold Spring Harb Perspect Biol 1:a002576. doi:10.1101/cshperspect.a002576

Harris AL (2007) Connexin channel permeability to cytoplasmic molecules. Prog Biophys Mol Biol 94:120–143. doi:10.1016/j.pbiomolbio.2007.03.011

Heinemann D, Schomaker M, Kalies S, Schieck M, Carlson R, Murua Escobar H, Ripken T, Meyer H, Heisterkamp A (2013) Gold nanoparticle mediated laser transfection for efficient siRNA mediated gene knock down. PLoS One 8:e58604. doi:10.1371/journal.pone.0058604

Kalies S, Birr T, Heinemann D, Schomaker M, Ripken T, Heisterkamp A, Meyer H (2014) Enhancement of extracellular molecule uptake in plasmonic laser perforation. J Biophotonics 7:474–482. doi:10.1002/jbio.201200200

Kalies S, Heinemann D, Schomaker M, Escobar HM, Heisterkamp A, Ripken T, Meyer H (2013) Plasmonic laser treatment for morpholino oligomer delivery in antisense applications. J Biophotonics. doi:10.1002/jbio.201300056

Ke Q, Li L, Cai B, Liu C, Yang Y, Gao Y, Huang W, Yuan X, Wang T, Zhang Q, Harris AL, Tao L, Xiang AP (2013) Connexin 43 is involved in the generation of human-induced pluripotent stem cells. Hum Mol Genet 22:2221–2233. doi:10.1093/hmg/ddt074

Kelsell DP, Dunlop J, Hodgins MB (2001) Human diseases: clues to cracking the connexin code? Trends Cell Biol 11(1):2–6

Lee C, Chen I, Lee C, Chi C, Tsai M, Tsai J, Lin H (2010) Inhibition of gap junctional intercellular communication in WB-F344 rat liver epithelial cells by triphenyltin chloride through MAPK and PI3-kinase pathways. J Occup Med Toxicol 5:17. doi:10.1186/1745-6673-5-17

Nielsen MS, Axelsen LN, Sorgen PL, Verma V, Delmar M, Holstein-Rathlou N (2012) Gap junctions. Compr Physiol 2:1981–2035. doi:10.1002/cphy.c110051

Osswald M, Winkler F (2013) Insights into cell-to-cell and cell-to-blood-vessel communications in the brain: in vivo multiphoton microscopy. Cell Tissue Res 352:149–159. doi:10.1007/s00441-013-1580-3

Schomaker M, Fehlauer H, Bintig W, Ngezahayo A, Nolte, I, Murua-Escobar, H, Lubatschowski H, Heisterkamp A (2010) Fs- laser cell perforation using gold nanoparticles of different shapes. Proceedings of SPIE 7589:75890C-75890C-5

Schomaker M, Killian D, Willenbrock S, Heinemann D, Kalies S, Ngezahayo A, Nolte I, Ripken T, Junghanss C, Meyer H, Escobar HM, Heisterkamp A (2014) Biophysical effects in off-resonant gold nanoparticle mediated (GNOME) laser transfection of cell lines, primary- and stem cells using fs laser pulses. J Biophotonics 9999. doi:10.1002/jbio.201400065

Stevenson D, Gunn-Moore F, Campbell P, Dholakia K (2010) Transfection by optical injection. In: Tuchin V (ed) Handbook of photonics for biomedical science. CRC Press, Taylor and Francis Group, London, pp. 87–118

Werkmeister E, Kerdjoudj H, Marchal L, Stoltz JF, Dumas D (2007) Multiphoton microscopy for blood vessel imaging: new non-invasive tools (Spectral, SHG, FLIM). Clin Hemorheol Microcirc 37(1–2):77–88

Willecke K, Eiberger J, Degen J, Eckardt D, Romualdi A, Guldenagel M, Deutsch U, Sohl G (2002) Structural and functional diversity of connexin genes in the mouse and human genome. Biol Chem 383:725–737. doi:10.1515/BC.2002.076

Xia Y, Gong K, Xu M, Zhang Y, Guo J, Song Y, Zhang P (2009) Regulation of gap-junction protein connexin 43 by beta-adrenergic receptor stimulation in rat cardiomyocytes. Acta Pharmacol Sin 30:928–934. doi:10.1038/aps.2009.92

Zoidl G, Dermietzel R (2010) Gap junctions in inherited human disease. Pflügers Arch. 460:451–466. doi:10.1007/s00424-010-0789-1